



Disentangling the impacts of exogenous disturbances on forest stands to assess multi-centennial tree-ring reconstructions of avalanche activity in the upper Goms Valley (Canton of Valais, Switzerland)



Adrien Favillier^{a, *}, Sébastien Guillet^{b, c}, Pauline Morel^{b, c, d}, Christophe Corona^a, Jérôme Lopez Saez^d, Nicolas Eckert^e, Juan Antonio Ballesteros Cánovas^{b, c}, Jean-Luc Peiry^{a, f}, Markus Stoffel^{b, c}

^a Université Clermont Auvergne, CNRS, GEOLAB, F-63000 Clermont-Ferrand, France

^b University of Geneva, Institute for Environmental Sciences, Climatic Change and Climate Impacts, 66 Boulevard Carl-Vogt, CH-1205 Geneva, Switzerland

^c Dendrolab.ch, Department of Earth Sciences, University of Geneva, rue des Maraîchers 13, CH-1205 Geneva, Switzerland

^d UR EMGR, Irstea/Université Grenoble Alpes, 38402 St-Martin-d'Hères cedex, France

^e UR ETNA, Irstea/Université Grenoble Alpes, 38402 St-Martin-d'Hères cedex, France

^f CNRS, UMI3189, (Environnement, Santé, Sociétés), Faculté de Médecine, UCAD, BP 5005, DAKAR-FANN, Senegal

ARTICLE INFO

Article history:

Received 25 April 2017

Received in revised form

17 August 2017

Accepted 3 September 2017

Available online 6 September 2017

Keywords:

Dendrogeomorphology

Snow avalanches

Spatio-temporal analysis

Tree ring

Swiss Alps

ABSTRACT

The purpose of dendrogeomorphic analyses is to amplify the signal related to the geomorphic process under investigation, and to minimize the noise induced by other signals in the tree-ring series. Yet, to date, no study accounts specifically for interferences induced by climate conditions or exogenous disturbances and which can, potentially, affect the quality of tree-ring based process reconstructions. In this paper, we develop a specific procedure allowing evaluation of the quality of reconstructions in five avalanche paths at Oberwald (Swiss Alps). The study is based on possible interferences between snow avalanches, climatic conditions and ecological signals in the tree-ring series. Analysis of past events was based on tree-ring series from 564 heavily affected, multi-centennial European larch trees (*Larix decidua* Mill.) growing near or next to the avalanche paths. A total of 2389 growth disturbances, such as scars, tangential rows of traumatic resin ducts, compression wood as well as abrupt growth suppressions or releases, were identified in the samples, indicating 43 destructive snow avalanches since AD 1780. At the same time, 31 potential events, which were detected with the conventional *Shroder* index value, were rejected from the final reconstruction due to potentially strong interferences between the different signals. This high rejection rate underlines the necessity to systematically—and carefully—discriminate ecological and climatic noise from avalanche-related disturbances. This discrimination is even more so crucial as a significant proportion of dendrogeomorphic studies in the Alps are based on *L. decidua* trees which are cyclically affected by larch budmoth outbreaks.

© 2017 Elsevier B.V. All rights reserved.

1. Introduction

Snow avalanches are a major natural hazard in the Alps. Every year, they affect transport infrastructure and may endanger settlements and threaten human life. Over the last century, urban sprawl in mountain areas in combination with a growing demands for mobility and recreational activities have increased avalanche

risk significantly. Substantial efforts have therefore been deployed to build databases with past avalanche events so as to provide accurate information regarding their magnitude, spatial extent, and return period. However, historic documentation of past avalanche activity is most often biased toward events that caused damage to infrastructure or loss of life, and remains largely nonexistent in sparsely or recently populated areas (Corona et al., 2012). On forested paths, dendrogeomorphology (Alestalo, 1971; Stoffel et al., 2010) has proven to compensate for the scarcity of written sources as it allows reconstruction of past, natural avalanche activity in time and space (Butler and Sawyer, 2008). The approach, first

* Corresponding author. GEOLAB UMR 6042, 4 rue Ledru, 63057 Clermont-Ferrand CEDEX 1, France.

E-mail address: adrien.favillier@uca.fr (A. Favillier).

elucidated by Alestalo (1971), takes advantage of the fact that trees growing in temperate climates do not only form yearly increment rings, but that they will also record the occurrence of external disturbance events in their growth-ring series, thus allowing accurate dating and reconstruction of past process histories (Stoffel and Corona, 2014).

Cook (1987) described the tree growth as a linear aggregate of several unobserved subseries following:

$$R_t = A_t + C_t + \delta D_{1t} + \delta D_{2t} + E_t$$

where R_t is the observed ring-width series; A_t is the age-size related trend in ring-width; C_t is the climatically related environmental signal; δD_{1t} is the disturbance pulse caused by a local endogenous disturbance; δD_{2t} is the disturbance pulse caused by a stand-wide exogenous disturbance; and E_t is the largely unexplained year-to-year variability not related to the other signals.

The purpose of dendrogeomorphic approaches therefore is to amplify the parameter δD_{1t} related to the process under investigation (i.e. snow avalanches) and to minimize the noise induced by other signals. The reconstruction of snow avalanching using tree rings has a fairly long history with increasing sophistication characterizing most recent applications (Butler and Sawyer, 2008). Since the seminal reconstructions of Potter (1969) and Schaerer (1972) in North America, new growth disturbances, such as tangential rows of traumatic resin ducts (referred hereafter as TRDs), have been added to more classical parameters (Stoffel et al., 2005; Stoffel, 2008; Stoffel and Hitz, 2008; Schneuwly et al., 2009a,b). In addition, different quantitative approaches have been proposed so as to enhance the detection of snow avalanche years (Corona et al., 2012; Schläpky et al., 2013; Stoffel et al., 2013; Chiroiu et al., 2015; Germain, 2016; Martin and Germain, 2016a). Paradoxically, no single study has so far accounted specifically for the interferences which can be induced potentially by climatic conditions (C_t) or by exogenous disturbances (e.g., insect and pathogen attacks, fire, windstorms or anthropogenic influences) on the dendrogeomorphic reconstructions.

The purpose of this study therefore is to maximize the tree-ring signal related to past snow avalanches. To this end, we focused on (i) the dendrogeomorphic reconstruction of past snow avalanches in the upper Goms Valley (Canton of Valais, Swiss Alps), where long chronologies of past snow avalanche activity are lacking, despite the fact that massive events in 1998/9 have damaged substantially century-old forest stand and infrastructure; (ii) the disentangling of geomorphic signals in tree-ring series from climatic and ecological signals; (iii) a quantification of the reliability of each reconstructed event, based on the inclusion of information on historical events; and (iv) the qualitative magnitude of individual, past snow avalanche events.

2. Study site

The Oberwald avalanche paths (46°32'N, 8°20'E, Fig. 1) are located on the south-facing slope of the upper Goms Valley in the Central Swiss Alps (Canton of Valais, Switzerland, Fig. 1a–b). These paths threaten the village of Oberwald and the Matterhorn-Gotthard Bahn (MGB) railway line connecting Brig (Canton of Valais) to Andermatt (Canton of Uri) (Fig. 1c). The site under investigation is 155 ha in size and has a difference in elevation of about 820 m (1360–2180 m asl) from the base of the slope to the highest release zones. Its geology is dominated by biotite gneisses interrupted by granitic cliffs oriented E-W (Federal Office of Topography Swisstopo). Two main channels, i.e. the Rätischbach and one of its unnamed tributaries, have witnessed recent snow avalanche activity leaving a 260-m wide cone at the foot of the

Rätischbach avalanche path.

According to data from the nearby meteorological station at Ulrichen (46°5'N, 8°31'E, 1346 m asl), annual temperature is 3.7 °C for the period 1981–2010 and annual precipitation amounts to 1212 mm. During winter, mean air temperature (DJF) is –6.6 °C and between November and April precipitation falls primarily as snow with average annual snowfall reaching 578 cm for the period 1999–2010 (the average snow cover period is 171 days). Snow avalanches release spontaneously at the site from a series of starting zones located between 1680 and 2200 m asl. Once released, they pass through a forested slope mainly composed of European larch (*Larix decidua* Mill.) and Norway spruce (*Picea abies* (L.) Karst.). Archival records report several avalanche events (section 3.1) since AD 1720 and the structure of the forest stand points to repeat and ongoing avalanche activity at the site to the current day. As a consequence, several rows of deflecting barriers have been put in place by the state authorities to stabilize snowpack in the source area of avalanches and to prevent the release of avalanches (Fig. 1).

3. Material and methods

3.1. Compilation of historical archives

First, we compiled a historical database of past snow avalanches at Oberwald based on different documentary sources available for the period 1900–2013 at the *Institut zur Erforschung der Geschichte des Alpenraums* (FGA) and from the local forest service. For this period, documentation was also extracted from technical reports established by the Swiss Federal Institute for Snow and Avalanche Research (SLF) and from local newspapers. Before the 20th century, local chronicles available at FGA and information contained in the Swiss database from Laternser and Pfister (1997) were reviewed in detail. To complement the archival database, six aerial flight campaigns available from the Federal Office of Topography (swisstopo; in the scale of ca. 1:20,000) were used in addition so as to detect evidence of damaging avalanche events since 1946.

3.2. Delineation of avalanche path

Several factors render a precise delineation of the avalanche flow paths at Oberwald rather complex, namely (i) the multitude of release areas, (ii) the absence of preferential paths in the western part of the slope and (iii) the dense forest cover, which is effectively masking geomorphic evidence of past avalanche events. To overcome this limitation, we used the numerical avalanche dynamics model RAMMS (*Rapid Mass Movement System*; Gruber and Bartelt, 2007; Christen et al., 2010), as it has proven to be useful for an accurate delineation of flow paths in complex terrain (Rudolf-Miklau et al., 2015). RAMMS predicts avalanche runout distances, flow velocities, impact pressures and a three-dimensional terrain model using a finite volume scheme to solve the shallow water equations. The required input parameters for RAMMS include (i) a digital elevation model (DEM), (ii) information about the size and location of the release area and snow height in the release area, as well as (iii) friction parameters. The simulations with RAMMS were based on a 1-m Digital Elevation Model (DEM) provided by the Canton of Valais. The spatial extent of avalanche release areas as well as the previously recognized hazard areas was determined based on expert knowledge (Fig. 1c). Paths were delineated based on return periods (30, 100 and 300 years) and the maximal extent of pressure output data given by the simulations.

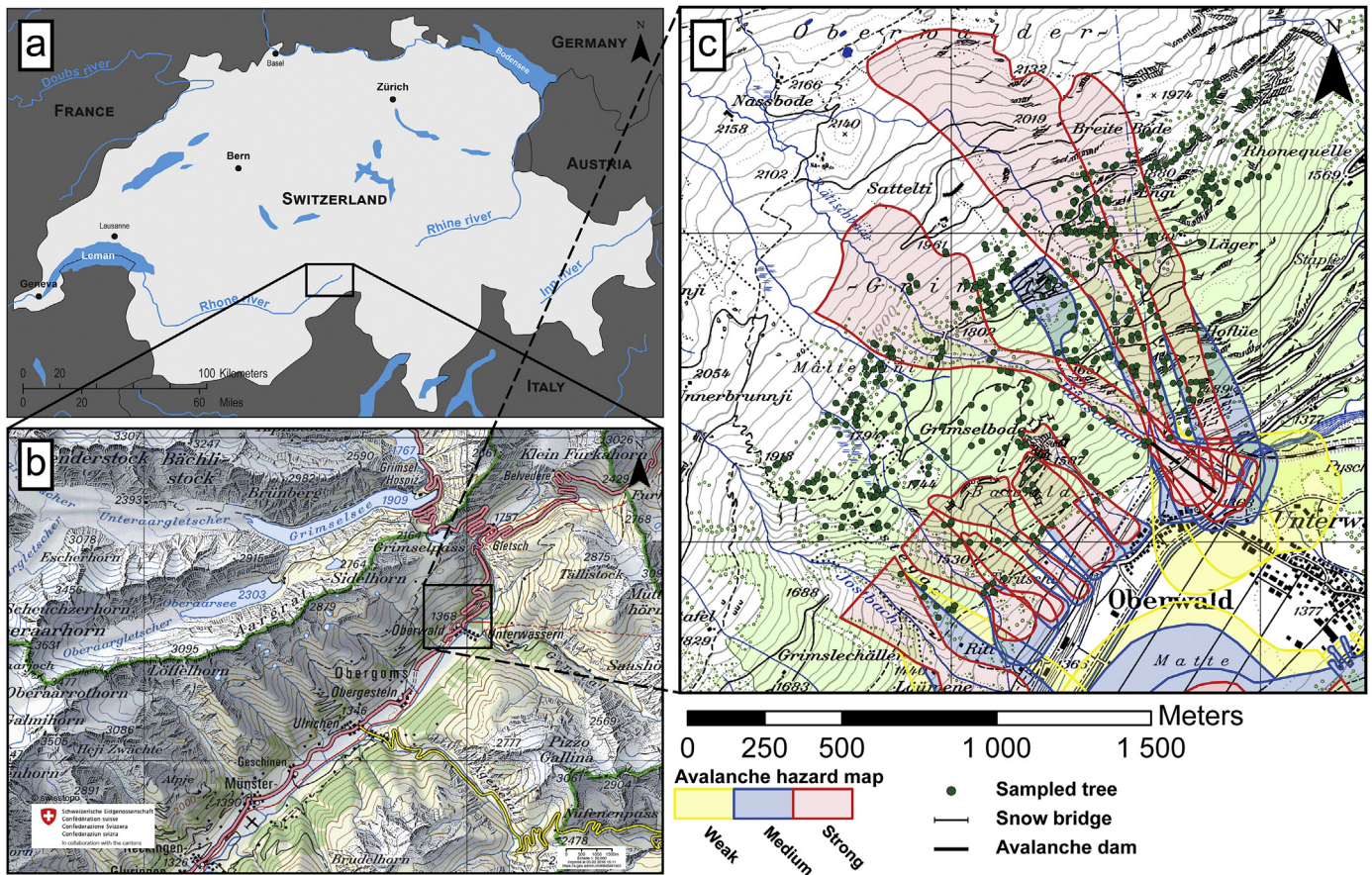


Fig. 1. Location of the study site in (a) Switzerland and (b) in the Goms Valley. (c) Spatial distribution of sampled trees. The colored areas represent the hazard map defined by the canton of Valais. Red indicates an area that is exposed to considerable danger with frequent avalanches (average return period of 30 years or less). In the blue colored area, avalanches are less frequent (30–100 year average return period) and have mean pressures of less than 30 kN/m². The yellow area is giving the extent of avalanches with return periods of 100–300 years, but also designates the runout zone of powder avalanches. (For interpretation of the references to colour in this figure legend, the reader is referred to the web version of this article.)

3.3. Sampling strategy, identification, dating and classification of growth disturbances

To reconstruct past avalanche activity based on dendrogeomorphic techniques, a total of 1140 increment cores and 10 cross-sections were sampled from 564 of European larch (*Larix decidua* Mill.) and Norway spruce (*Picea abies* (L.) Karst.) trees using Pressler increment borers (diameter 5.15 mm, maximum length 40 cm) in summers 2013 and 2014. A minimum of two cores was extracted per tree, one perpendicular to the slope and one in the downslope direction. Additional data were collected for each tree including its diameter at breast height, description of the disturbance (i.e. amount of scars, decapitation, tilting), exact position of the sampled tree using a 1-m precision GPS device and data about neighboring trees.

Trees presenting obvious evidence of snow avalanches, such as decapitation, tilting, and injury, were preferentially selected. Following recent recommendations by Stoffel and Corona (2014), old trees were selected to extend the reconstruction of past avalanche events as far as possible. Nevertheless, younger trees were also considered to account for the loss of sensitivity of older trees in recording mass-movement signals (Šilhán and Stoffel, 2015). Sampling height was chosen according to the morphology of the stem: (i) injured trees were sampled at the height of the disturbance from the overgrowing scar tissue; (ii) tilted tree samples were extracted at the maximum bending angle (Stoffel et al.,

2013); (iii) cross-sections and cores from decapitated trees were taken at the lowest possible position on the tree to maximize the number of available rings (Stoffel and Bollschweiler, 2008). Samples were prepared and data processed following standard procedures described in Stoffel et al. (2013). Growth disturbances (GD) such as impact scars and callus tissues (CT) (Stoffel et al., 2010), tangential rows of traumatic resin ducts (TRD) (Schneuwly et al., 2009a,b), compression wood (CW) and abrupt growth suppression (GS; Kogelnig-Mayer et al., 2013) were identified in the tree-ring series and cross-dated with two local reference chronologies (Büntgen et al., 2005), so as to correct our series for possibly missing rings.

Intensities were then assigned to each GD using criteria defined by Kogelnig-Mayer et al. (2011). This step was included to emphasize features which were clearly associated with avalanche activity. The intensities of growth suppression, compression wood, and TRDs were classified according to Schneuwly et al. (2009a,b) and Frazer (1985) to distinguish between weak (intensity class 1), medium (intensity class 2), and strong (intensity class 3) reactions and clear evidence of injuries (intensity class 4).

3.4. Detection of past avalanche events in growth disturbance series

To detect past snow avalanches in the GD series and to disentangle potential effects of snow avalanches from disturbance pulses caused by climatic or exogenous factors, such as drought years or

larch budmoth outbreaks, a four-step procedure was adopted in this study. The approach indeed combines the avalanche event detection methods developed by Shroder (1978), Reardon et al. (2008), Kogelnig-Mayer et al. (2011) and Corona et al. (2012).

- (i) In a first step, for each year t and for each path, an index I was calculated, according to Shroder (1978); this index is based on the percentage of trees showing responses in their growth ring record in relation to the number of sampled trees being alive in year t:

$$I_t = \left(\left(\sum_{i=1}^n R_t \right) / \left(\sum_{i=1}^n A_t \right) \right) * 100$$

where $\sum R$ represents the number of trees responding to an event in year t, and $\sum A$ is the number of trees alive in year t. Following recommendations from Butler and Sawyer (2008), a double threshold for sample sizes of 21–54 ($GD > 4$ and $I_t > 5\%$) and ≥ 55 trees ($GD > 7$ and $I_t > 5\%$) has been used to discriminate potential avalanche and non-avalanche years in accordance with statistically determined thresholds as defined by Corona et al. (2012) for the Pèlerins avalanche path (France). These thresholds also aimed at limiting the inclusion of noise related to snow creeping (Stoffel and Corona, 2014), snow loading (Martin and Germain, 2016a), or any other kind of ecological disturbances (Butler and Sawyer, 2008; Corona et al., 2012) in the process reconstruction (Fig. 2).

- (ii) The grey larch budmoth (LBM, *Zeiraphera diniana* Gn.) is a foliage feeding Lepidopteran insect responsible for periodical outbreaks (8- to 10-year intervals), mainly in the interior valleys of the European Alps (Baltensweiler et al., 1977). The feeding of the LBM on larch needles causes massive defoliation resulting in growth suppression lasting over 3–4 years (Kress et al., 2009) which may, thus, interfere with the dendrogeomorphic signal contained in tree rings. In total, 21

triplets of LBM outbreak years (i.e. series of three consecutive years, Table 1) have been reconstructed in the Swiss Alps since 1780 according to Esper et al. (2007) and Büntgen et al. (2009). Similarly, climate extremes such as cold summers and prolonged droughts are susceptible of durably affecting larch growth (Battipaglia et al., 2010; Lévesque et al., 2013; George et al., 2016) and to cause prolonged growth suppressions that may be assimilated to avalanche-related GDs. According to Battipaglia et al. (2010), in the central Alps, extremely cold summers were recorded in tree-ring data and historical archives in 1814, 1816, 1829, 1833, 1851, 1860, 1896, 1912, 1924, 1964, 1972, 1984, and 1995. Based on the gridded HISTALP point temperature information (Efthymiadis et al., 2006) closest to the study site, 14 years with negative May–September anomalies of precipitation (with values exceeding–1.5 SD below the average) could be found for the period 1800–2003—and have thus been considered as dry years (Table 1).

Potential avalanche events detected in step 1 coinciding with

Table 1

Larch budmoth events (according to Esper et al., 2007; Büntgen et al., 2009), as well as extremely cold and dry summers (Efthymiadis et al., 2006) in the Swiss Alps. All these years have been carefully analyzed due to probable interferences between snow avalanche damage in trees, as well as LBM and climatic signals.

2003	1965	1924	1888	1830
1995	1963	1923	1880	1829
1989	1962	1919	1871	1821
1986	1959	1915	1870	1816
1984	1954	1912	1864	1814
1981	1945	1908	1860	1811
1976	1937	1906	1856	1801
1972	1931	1896	1851	1792
1972	1929	1896	1838	1779
1966	1928	1895	1833	1771

LBM-outbreak years, Extreme cold summer, Drought years.

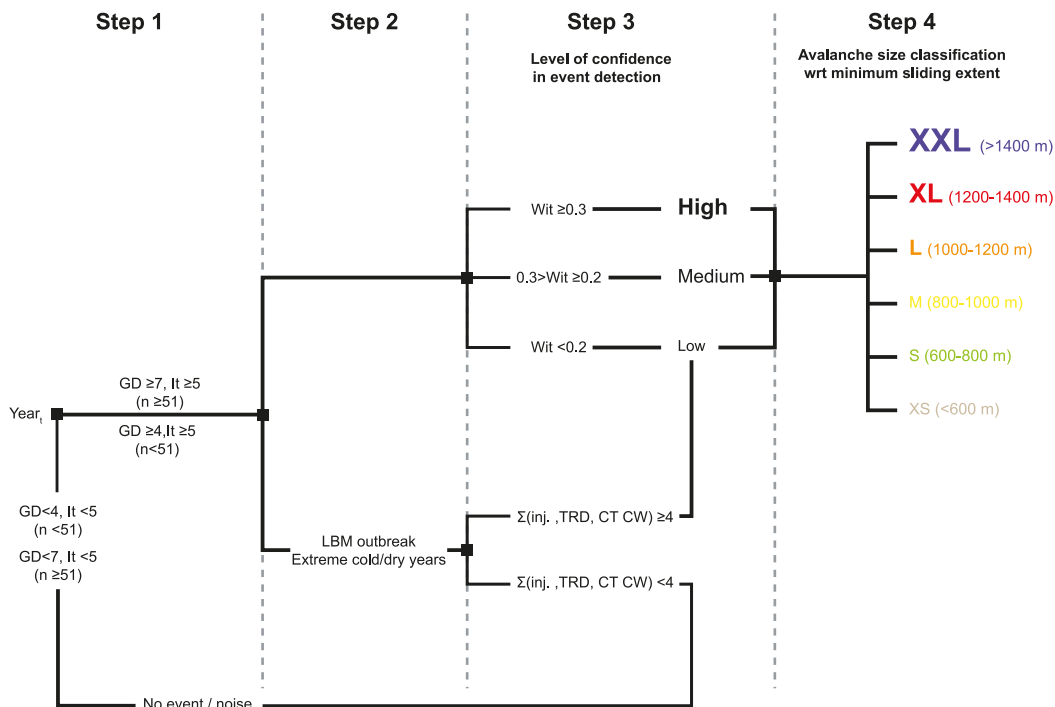


Fig. 2. Synoptic diagram of the 4-step approach used for the detection of avalanche events in tree-ring series.

LBM outbreak episodes or extremely cold/dry years were therefore examined in more detail. In order to limit possible interferences between geomorphic, climatic, and LBM signals, growth suppressions were systematically excluded from the account of GDs and a minimum threshold of 4 GDs was retained to discriminate avalanche from non-avalanche years (Fig. 2).

(iii) In a third step, the type and intensity of GDs were used to evaluate a qualitative level of confidence associated with the detection of each reconstructed event. To this end, a weighted index factor (Wit), adapted from Kogelnig-Mayer et al. (2011), was computed for each avalanche event detected in step 1 as follows:

$$W_{it} = \frac{[(\sum_{i=1}^n T_i * 7) + (\sum_{i=1}^n T_s * 5) + (\sum_{i=1}^n T_m * 3) + (\sum_{i=1}^n T_w * 1)]}{\sum_{i=1}^n A_t}$$

where, for each year t, T_i represents the sum of trees with injuries; T_s represents the sum of trees with strong GDs; T_m represents the sum of trees with medium-intensity GDs; T_w represents the sum of trees with weak-intensity GDs, and where A gives the total number of trees alive in year t. Based on the Wit, we then distinguish between low (LLC, $Wit < 0.2$), medium (MLC, $0.3 > Wit > 0.2$), and high (HLC, $Wit > 0.3$) levels of confidence and attribute this evaluation to the avalanche event detection. In addition, and despite the precautions taken at each of the previous step, each event detected at step 2 was rated with a LLC (Fig. 2).

(iv) Finally, avalanche years and corresponding GDs were mapped using the ArcGIS 10.2 Time Slider (Kennedy, 2013; ESRI, 2013) so as to estimate the minimum sliding extent (ME, w.r.t the barycenter of the avalanche release zones) of each avalanche event. On the basis of ME, avalanche events with $ME < 600$, $600 < ME < 800$, $800 < ME < 1000$, $1000 < ME < 1200$, $1200 < ME < 1400$ and $ME > 1400$ were classified as eXtra Small (XS), Small (S), Medium (M), Large (L), eXtra Large (XL), and eXtra eXtra Large (XXL) events, respectively.

The age structure of the stand was approximated by counting the number of tree rings in the selected trees and was visualized after interpolation. However, since trees were not sampled at their stem base and as piths as well as the innermost rings of some trees were rotten, the age structure does neither reflect inception nor germination dates. Nonetheless, this data may provide valuable insights into major disturbance events at the study site with reasonable precision, as *L. decidua* has been shown repeatedly to recolonize surfaces cleared by snow avalanches or other mass-movement processes in the years following an event (Stoffel et al., 2006; Van der Burght et al., 2012).

For each path, the annual probability for an avalanche event was computed as:

$$AP_i = \left(\frac{A_i}{L_i} \right)$$

where A represents the number of reconstructed events at path i and L is the period covered by the reconstruction at site i.

4. Results

4.1. Mapping of avalanche path at Oberwald

At Oberwald, precise geomorphic mapping—including field

observations and a digital terrain model (DTM) generated from airborne Lidar data point clouds—as well as flow extensions with the RAMMS numerical snow avalanche simulations revealed a minimum of five distinct avalanche paths, namely from east to west: OB1 (57.8 ha, 1258 m long, 611 m wide), OB2 (66.6 ha, 1578 m long, 532 m wide), OB3 (39.15 ha, 1845 m long, 318 m wide), OB4 (29.63 ha, 1364 m long, 344 m wide), and OB5 (38.19 ha, 1141 m long, 377 m wide) (Fig. 3).

4.2. Snow avalanches recorded in historical archives

For the period AD 1780–2017, six events were found in local archives, namely in 1921, 1935, 1951, 1961, 1999, and 2003. During winter 1950–51, an extreme avalanche occurred at Rätischbach (OB3).

4.3. Age structure of the stand

In total, 564 European larch (*Larix decidua* Mill.) and Norway spruce (*Picea abies* (L.) Karst.) trees were sampled with 1140 increment cores and 10 cross-sections. The samples were distributed as follows between the five paths: OB1: 127 trees, OB2: 135 trees, OB3: 100 trees, OB4: 125 trees, and OB5: 77 trees. After cross-

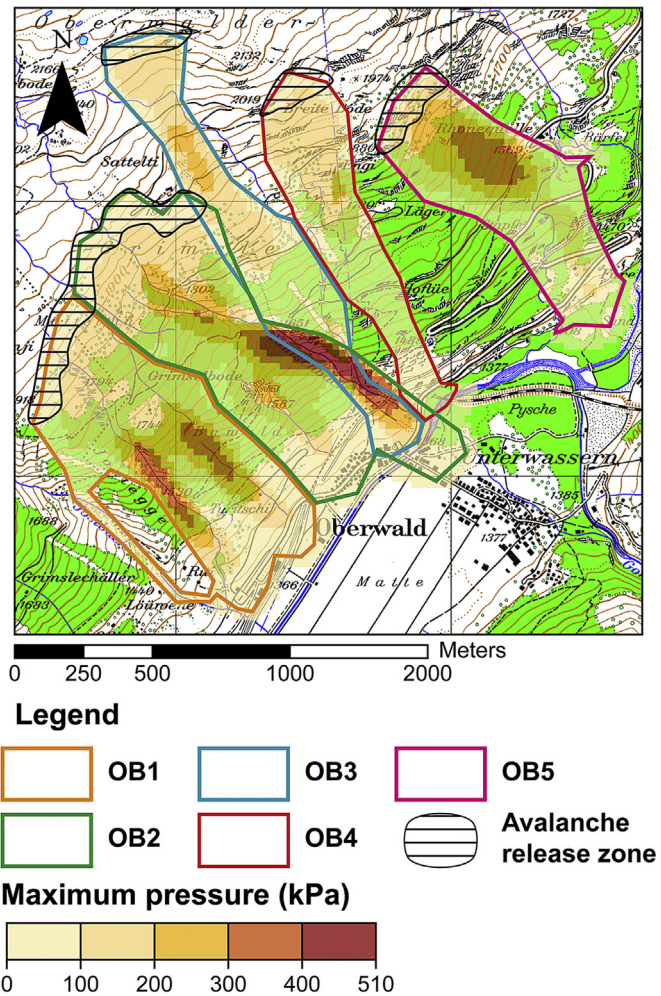


Fig. 3. Mapping of the avalanche paths (OB1–OB5) at Oberwald based on field observations and digital terrain model (DTM) data derived from airborne Lidar data point clouds, as well as maximal extension of avalanche flows as derived from maximal pressure data from RAMMS numerical snow avalanche simulations.

dating, data on the pith age at breast height indicates that European larch and Norway spruce trees growing at Oberwald were on average 206 yrs old (± 115 yrs). The oldest tree selected for analysis attained sampling height in AD 1429 while the youngest tree only reaches breast height in AD 1991. As illustrated in Fig. 4, the stand is dominated by 100–200-yr (37.1%) and 200–300-yr (27.8%) old trees. In total, 39 and 13 trees could be found with ages exceeding 400 years and 500 years, respectively. Young trees (≤ 100 yr, 16.8%) are scattered over the slope and do not show any significant pattern which would suggest forest recolonization after high-magnitude disturbance events. By contrast, the oldest trees are preferentially located in two patches located above 1800 m a.s.l., on the interfluvial of OB1/OB2 and OB2/OB3, thus suggesting that no event in the recent past would have had sufficient energy to completely destroy these forest stands over the last centuries.

4.4. Distribution of growth disturbances

Sampled cores and cross-sections permitted identification of 2389 GD in the tree-ring series, 489 of which were considered strong avalanche indicators (Class 3 or 4). Table 2 summarizes the types of GD as well as their intensity. TRDs, CT and CW were the GDs most frequently (54.5%) identified in the samples, followed by growth suppressions (GS; 43.6%). By contrast, only 47 injuries were sampled, which represents 1.9% of the dated disturbances. In total, 51.2% of the GDs were rated as intensity 1 and 28.3% as intensity 2. Intensities 3 and 4 represent 18.5% and 1.9% of detected GDs, respectively. The oldest GD identified in the tree-ring series was dated to AD 1781. GDs are more frequent after AD 1900 and nearly

Table 2

Intensity of reactions and types of growth disturbances (GD) assessed in the 564 larch trees selected for analysis.

Intensity	1	2	3	4	Total
Injuries	–	–	–	47 (1.9%)	47 (1.9%)
CT, TRD	704 (29.5%)	313 (13.1%)	284 (11.9%)	–	1301 (54.5%)
GS	520 (21.8%)	363 (15.2%)	158 (6.6%)	–	1041 (43.6%)
Total	1224 (51.2%)	676 (28.3%)	442 (18.5%)	47 (1.9%)	2389 (100%)

every year exhibited GD in a small number of trees (Fig. 5).

GDs are almost evenly distributed between the five paths (OB1: 26.6%, 4 GD.tree⁻¹; OB2: 21.8%, 3.1 GD.tree⁻¹; OB3: 16.9%, 3.3 GD.tree⁻¹; OB4: 21.9%, 3.4 GD.tree⁻¹; OB5: 12.8%, 3.2 GD.tree⁻¹). A clear temporal trend is observed in the 50-yr distribution of GDs (Fig. 6), with an increasing frequency of TRD, CW, and CT since AD 1800 and an overrepresentation of injuries during the last 50 years. Conversely, the proportion of GS in the spectra of GDs continuously decreased from 46.7% for the period 1800–1850 to 17.5% after 1950.

4.5. Chronology of avalanche events

The event-response histogram depicted in Fig. 5 shows all reactions recorded in the trees along the avalanche paths. On the basis of our 4-step-procedure (Figs. 2 and 7), tree-ring analyses allowed reconstruction of 43 avalanche events between 1780 and 2013 (Fig. 9), with the oldest event being recorded in 1795 (OB1–OB4), and the most recent one in 2012 (OB1). Despite the exclusion of GS which were obviously related to LBM outbreaks or climatic extremes (step 2), the spectra of GDs used to reconstruct these events show a clear overrepresentation of TRD, CW, CT, and injuries during the last 100 years (Fig. 6b).

In total, 11 (1795–2012), 9 (1935–2003), 8 (1846–2005), and 15 (1795–2003) avalanche events were reconstructed at sites OB1–OB4, respectively. No event was reconstructed at site OB5. Based on possible interferences between the avalanche, climatic, and LBM signals in the tree-ring series (step 2), and on the basis of the Weighted Index Factor (Wit; step 3, Fig. 8) that accounts simultaneously for the type and intensities of GDs, we assigned high and medium levels of confidence to 5 and 7 events, respectively (see for example Fig. 10a and b). By comparison, 31 events with a Wit < 0.2, and characterized by a majority of weak and medium GDs, were therefore reconstructed with a LLC (Figs. 9 and 10b, e). Amongst the 42 potential events that coincide with LBM outbreak episodes or extreme climatic years, 31 were excluded from the reconstruction (Figs. 9 and 10f), and 11 were rated with a LLC (Table 3, Figs. 7 and 10e).

Higher levels of confidence were assigned to events that occurred at OB3 (2 HLC and 4 MLC events) and OB4 (3 HLC and 2 MLC events). Tree-ring signatures related to past snow avalanche activity were, by contrast, less frequent and less intense at sites OB1 and OB2, and a large majority of events (95%) was considered to have a LLC. Tree-ring evidence for the historical events in 1935, 1999, and 2003 could be identified at tracks OB1/OB2, OB2/OB3, and OB2/OB3/OB4, respectively. By contrast, an insufficient number of GDs and/or possible interferences with LBM outbreaks and climatic extremes prevented reconstruction of the documented snow avalanches in winters 1920/21, 1950/51, and 1960/61.

With respect to the 1780–2013 period and at the level of the slope scale, the mean frequency of snow avalanches is 1.87 events decade⁻¹. The reconstruction is characterized by a clear increase in avalanche frequency from 0.75 (9 events) to 3.1 events decade⁻¹ (34 events) for the periods 1780–1900 and 1901–2013, respectively. Maximum decadal frequencies are observed between 1951 and 1960 (5 events), 1991–2000 (6 events), and 2001–2013 (7

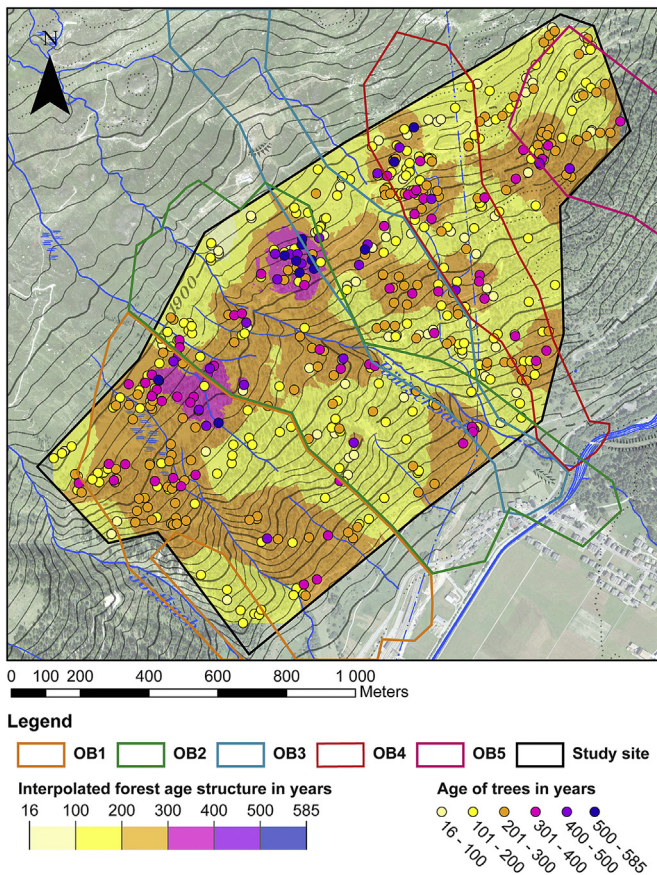


Fig. 4. Age structure of the forest stand growing in and next to the Oberwald avalanche paths.

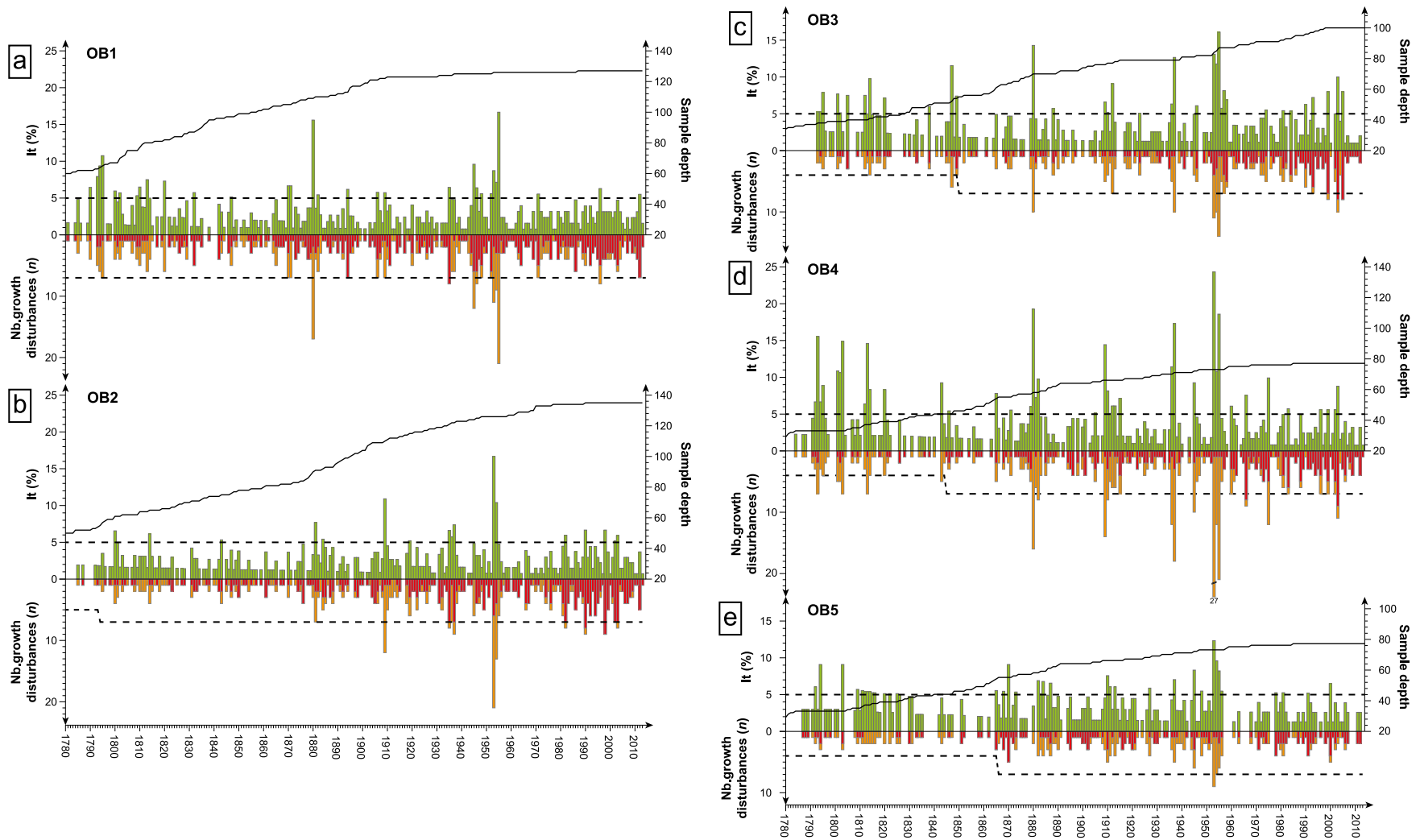


Fig. 5. Event-response histograms showing the total number of growth disturbances (GD, in red and orange) and the percentage of trees responding to an event (in green) at each of the five Oberwald paths (a–e). Orange bars show the total number of growth reductions which are possibly related to larch budmoth outbreaks or to climatic extremes. The dashed lines denote the GD and It thresholds used to reconstruct past avalanche events. The solid lines denote sample depth, i.e. the number of trees available for analysis for each year of the reconstruction. (For interpretation of the references to colour in this figure legend, the reader is referred to the web version of this article.)

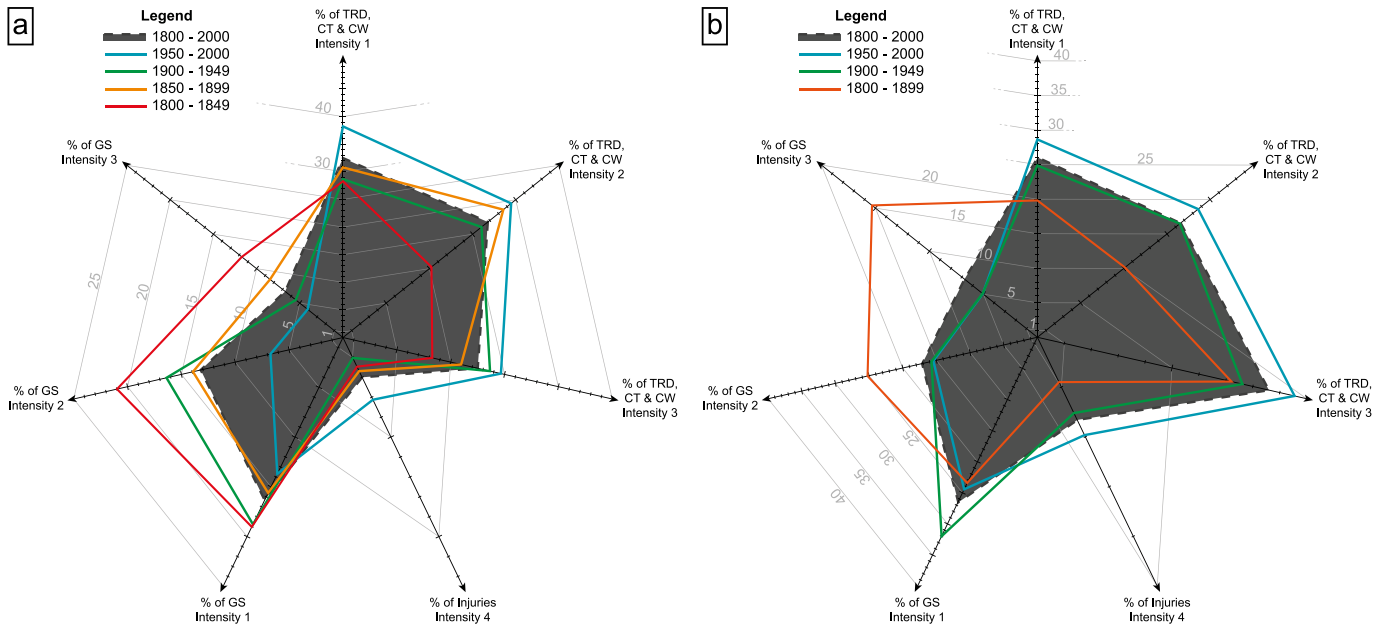


Fig. 6. Radar chart showing the distributions of GD types and intensities for 50-year periods between 1800 and 2000. Panel (a) includes all GD detected in trees, except during LBM outbreaks; panel (b) only shows GDs attributed to snow avalanche events.

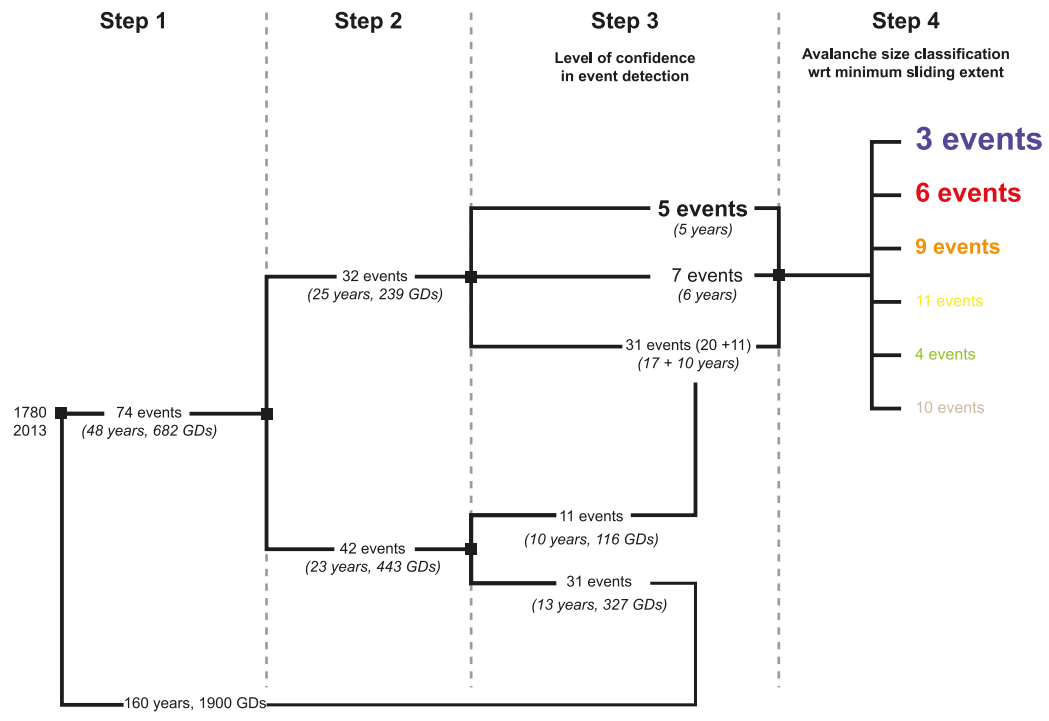


Fig. 7. Simplified synoptic diagram showing the characteristics (possible interference with climate or larch budmoth outbreaks, level of confidence, minimum slide extent) of the reconstructed events based on the 4-step procedure presented.

events). Conversely, no event was reconstructed for the periods 1780–1790, 1821–1834, 1831–1840, and 1851–1880. In more detail, the highest avalanche activity (16 events, amongst which 3 HLC and 4 MLC, 0.7 events decade⁻¹ since 1780) was observed at OB4, especially since 1960 (8 events, 1.6 events decade⁻¹). By comparison, OB2 is characterized by a much lower snow avalanche frequency (9 LLC events, 0.4 events decade⁻¹) and an asymmetric distribution of reconstructed avalanche events, i.e. no event until

1934 and 9 events between 1935 and 2013.

4.6. Spatial extent of avalanche events

In a final step, the spatial distribution of trees with GDs in a specific year has been used to estimate the minimum sliding extent (ME, w.r.t. to the barycenter of the release zones) for each reconstructed avalanche. In total, 18 out of the 43 (42%) reconstructed

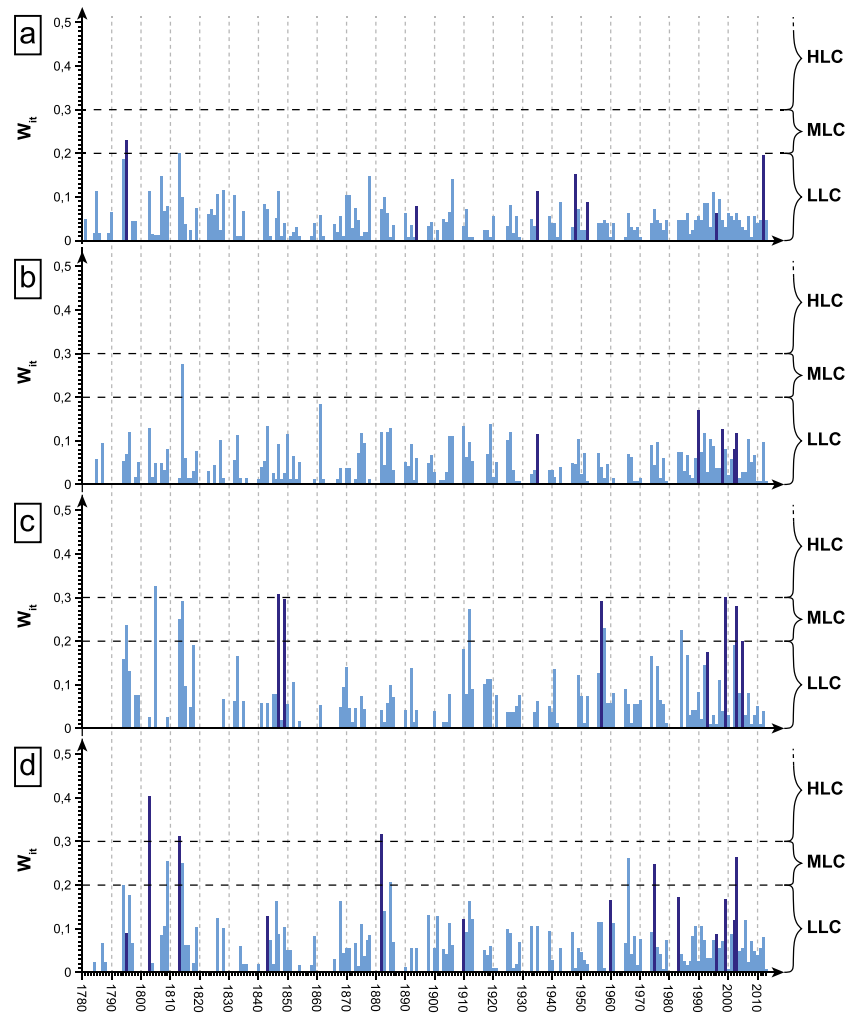


Fig. 8. Avalanche activity signals obtained with the weighted index factor (W_{it}) at (a) OB1, (b) OB2, (c) OB3 and (d) OB4. Light blue bars represent years rejected in step 1 and 2; dark blue bars denote avalanche years. (For interpretation of the references to colour in this figure legend, the reader is referred to the web version of this article.)

events exceed 1000 m in length and were thus classified as L (9), XL (6), or XXL (3) snow avalanches (Figs. 7 and 10a–d). Fourteen events, with a more limited slide extent ($ME < 800$), were classified as S. Eight of these events (1906-OB1, 1915-OB4, 1937-OB2, 1945-OB1, 1953-OB2-OB3 and 1971-OB1) coincide with a LBM outbreak or a drought year. As the number of GDs was ≥ 4 during these years, they were reintroduced in the final reconstruction at step 3 of our detection procedure but considered events with a LLC. Paradoxically, no clear relation was observed between the size of the event and the level of confidence associated to the reconstruction of each event: by way of example, among the 15 L-XL events, 9 were considered with a LLC. Similarly, among the four events considered with a HLC, two were of limited extent (M, 1803-OB4 and 1882-OB4), two exceeded 1200 m in length (XL, 1847-OB3 and 1999-OB3), but not a single avalanche was reconstructed as an extreme (XXL) event. Only three extreme events were reconstructed (1849-OB3, 2003-OB3 and 2005-OB3) and were considered with a MLC.

5. Discussion

5.1. Isolation of the avalanche signal in tree-ring series

The study we report here employs dendrogeomorphic

techniques for the analysis of snow avalanche activity on a complex forested slope located in the Valais Alps (Switzerland), with the aim of disentangling geomorphic signals in the tree-ring series (related to the occurrence of snow avalanches) from signals induced by other external disturbances. In addition, this study also aimed at estimating the robustness of tree-ring based snow avalanche reconstructions. To meet this objective, a detection procedure has been developed so as to include important methodological improvements achieved in the field of tree-ring based avalanche event detection over the last decade. This procedure therefore includes (i) a two-fold threshold with GDs and It that is varying according to the sample size (Corona et al., 2012; Stoffel et al., 2013) and which thus allows for a binary distinction between avalanche and non-avalanche years; (ii) local cyclic time series of insect outbreaks (Weber, 1997; Esper et al., 2007; Büntgen et al., 2009) and climatic extremes derived from existing reconstructions (Battipaglia et al., 2010; Efthymiadis et al., 2006) available for the Swiss Alps; and (iii) a weighted index that includes different response intensity classes (Germain et al., 2009; Kogelnig-Mayer et al., 2011) for the attribution of confidence levels to each of the detected snow avalanche events.

In a first step, 74 potential events were detected in the 1140 increment cores and 10 cross-sections sampled from *Larix decidua*

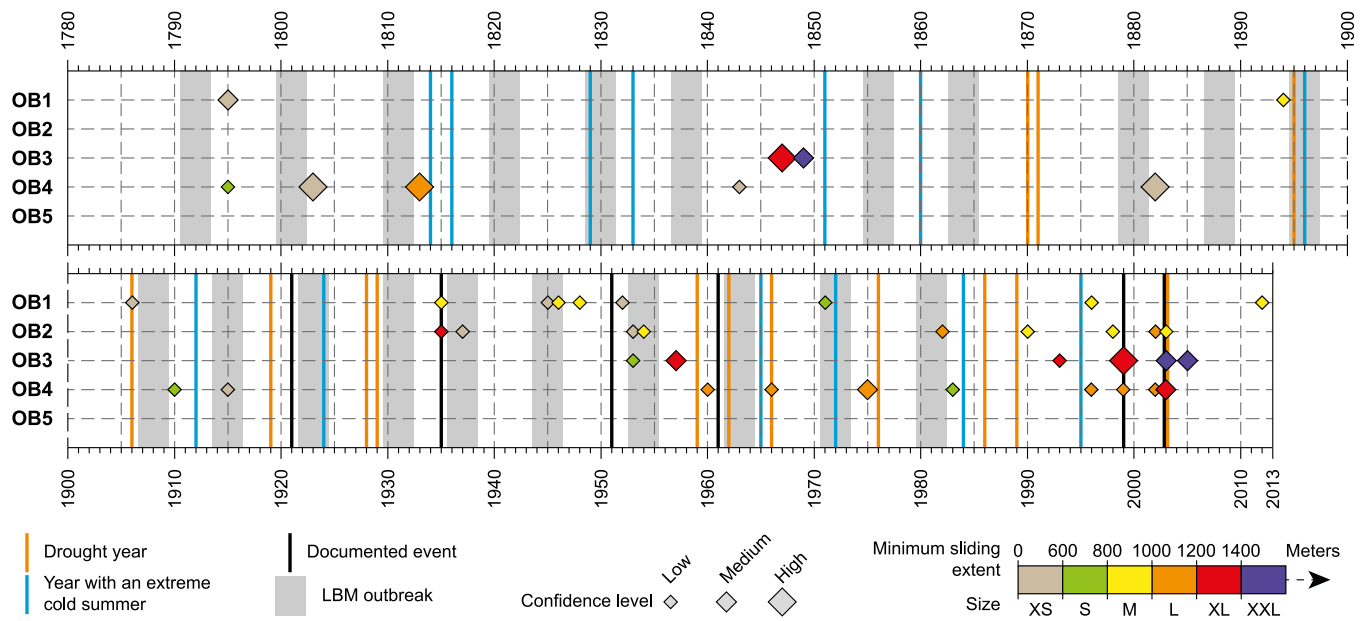


Fig. 9. Avalanche events reconstructed for the period 1780–2013 at the 5 avalanche paths. Symbol sizes are proportional to the level of confidence, whereas the color range denotes the minimum slide extent. Grey bands represent triplets of years associated to LBM outbreaks. Vertical lines show snow avalanche events documented in historical archives (black), as well as extremely dry (orange) and cold (blue) summers. (For interpretation of the references to colour in this figure legend, the reader is referred to the web version of this article.)

and *Picea abies* trees. Interestingly, from these potential events, 31 were excluded from analysis in step 2, despite the fact that they exceeded the It and GD thresholds. This exclusion was motivated by the fact that these 31 years (i) coincided with known larch budmoth outbreaks detected in the tree-ring series (Weber, 1997; Esper et al., 2007; Büntgen et al., 2009) or extremely cold/dry summers (Battipaglia et al., 2010; Efthymiadis et al., 2006) in the Swiss Alps; (ii) did not present a sufficiently large number of GDs (i.e. scars, callus tissue and to a lesser extent compression wood) that would have attested of clear impacts of avalanche events on the forest stand; and (iii) showed a scattered distribution of impacted trees across the slope which is not compatible with observed snow avalanche patterns. Although the approach presented here does not explicitly account for ecological disturbances such as windstorms—yet very frequent in Switzerland (Stucki et al., 2014), considered as one of the main damage factor to Swiss forests (Usbeck et al., 2009), and susceptible to interfere with the geomorphic signal in tree-ring series (Martin and Germain, 2016a)—the rejection rate (>40%) remains very high. As such, the approach presented here also highlights the necessity to discriminate avalanche signals from other ecological disturbances, especially in larch stands which are prone to cyclic LBM outbreaks.

The necessity of having these elements included in dendrogeomorphic assessments is not new and was previously postulated in methodological papers (Stoffel and Bollschweiler, 2008; Stoffel et al., 2013), but has only rarely been applied in dendrogeomorphic studies so far. This lack of consideration is even more critical as a significant proportion of tree-ring based snow avalanche studies—but also, and in a much broader perspective, dendrogeomorphic studies in general—have been based on larch trees (Table 4) which are known of being cyclically affected by larch budmoth (LBM) outbreaks. It is therefore possible that some noise may potentially have been included in reconstructions considering GDs other than injuries, callus tissues, TRDs and compression wood.

5.2. Robustness of the reconstruction

Based on the recent statistical testing of optimum sample sizes and noise reduction thresholds, there is scope and reason to assume that the event reconstructions emerging from our four-step procedure will indeed best reflect real avalanche activity at the Oberwald paths. In total, 3 out of 6 events listed in the testimonies were retrieved with dendrogeomorphic techniques. This success rate is comparable to tree-ring reconstructions of avalanches performed in the Oisans (Corona et al., 2010), Maurienne (Schläppy et al., 2013) and Mont-Blanc massifs (Corona et al., 2012). The most recent avalanche that occurred in 2003 at OB4 destroyed about 500 m³ of the forest stand and was successfully identified in our reconstruction. Its spatial extent is also very well captured by the tree-ring series, as can be seen from visual comparison between the two aerial photographs taken in 1999 and 2003 (Fig. 11).

Yet and despite the stringency of our approach for noise reduction as well as the substantial proportion of strong avalanche indicators (class 3 or 4) in the GD spectra—values are comparable to those obtained by e.g., Martin and Germain (2016a)—we realize that the robustness of our reconstruction remains quite low. Only 11 out of the 43 events detected in the tree-ring records (28%) were rated with a high or a medium level of confidence and a clear dichotomy exists in that regard between sites OB1/OB2 (5% of HLC/MLC events) and OB3/OB4 (45%).

At OB1/OB2, the over-representation of LLC events (95% of the reconstructed events) probably results from the scarcity of high-magnitude snow avalanche events. This hypothesis is supported by (i) the presence of the oldest trees (>300 years, Fig. 4) in the upper part of both couloirs, which suggests that no catastrophic, high-energy event was able to destroy larger parts of the forest stand during at least the past three centuries, (ii) the smoother transversal profile of these paths which favors the occurrence of unconfined, rather than channelized, snow avalanches (Fig. 3) as well as the existence of several rows of protective deflecting

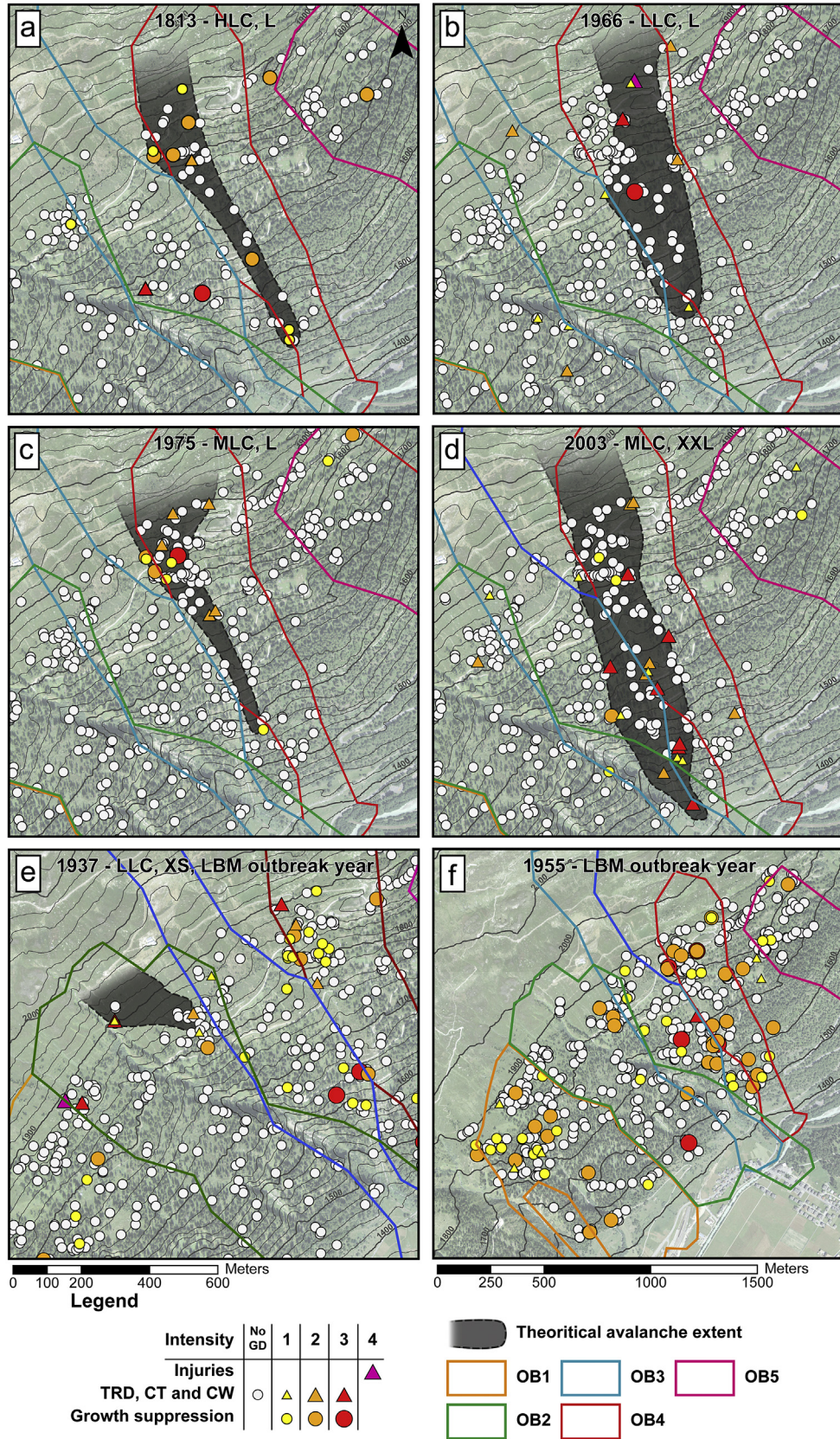


Fig. 10. Reconstructed minimum sliding extent for avalanches in (a) 1813, (b) 1966, (c) 1975, and (d) 2003; these events were reconstructed with high (HLC), medium (MLC) and low (LLC) level of confidence, respectively. Maps show all living trees and as well as those showing GDs related to the avalanche. Panels (e, f) are examples of events that were disregarded from the avalanche reconstruction due to the fact that geomorphic and LBM signals could not be disentangled in the tree-ring series.

Table 3
 Characteristics of reconstructed events coinciding with LBM outbreak episodes or extreme climatic events. The above events were retained in the final reconstruction due to their high proportion of strong GDs (i.e. callus tissue, injury, tangential rows and traumatic resin ducts, compression wood) which cannot be attributed to LBM outbreaks or climatic signatures. Nonetheless, events were rated with a low level of confidence due to probable interferences between the avalanche signals with growth suppressions induced by larch budmoth outbreaks and/or climatic extremes.

Years	External disturbance	Path	It (%)	GD	Number of injuries, CT, TRD and CW	Wit
1982	LBM outbreak	OB2	6.0	8	4	0.16
1971	LBM outbreak	OB1	5.6	7	5	0.13
1966	Drought	OB4	7.6	9	8	0.26
1954	LBM outbreak	OB2	10.4	13	4	0.23
1953	LBM outbreak	OB2	16.7	21	6	0.36
1953	LBM outbreak	OB3	13.1	11	4	0.25
1946	LBM outbreak	OB1	6.4	8	6	0.10
1945	LBM outbreak	OB1	9.6	12	6	0.16
1937	LBM outbreak	OB2	7.4	9	7	0.19
1915	LBM outbreak	OB4	7.1	7	4	0.19
1906	Drought	OB1	5.8	7	4	0.14

barriers which effectively prevented the release of high-magnitude events over the last decades.

At OB3, we hypothesize that the under-representation of HLC and MLC events would result (i) from the channelization of snow avalanches in deeply incised paths (Stoffel et al., 2010; Corona et al., 2012) and (ii) from the limitations of dendrogeomorphic techniques in such environments. In the best case, snow avalanches in such settings can be reconstructed via impacted trees standing at the outer lateral margins of the couloirs where impact energies are low and where trees are not necessarily affected during individual (smaller) events (Fig. 10a, b, c). Most often, avalanches located in or next to such couloirs will favor stem breakage—especially if (i) the bending stress exerted by the moving snow exceeds the bending strength of the tree stem (Johnson, 1987; Peltola et al., 1999) or if (ii) the applied torque overcomes the strength of the root-soil plate, leading to uprooting and overturning (Coutts, 1983). In this case, datable evidence of ancient events will be removed repeatedly and often almost systematically. This phenomenon is quite well exemplified by the snow avalanches which reportedly occurred at our site in the Jostbach and Rätischbach channels during the severe winter 1950–51 (Ancy, 2012). These events could not be retrieved from tree-ring records due to the lack of conifers growing in these channels and the widespread occurrence of young and flexible broadleaved trees (*Alnus viridis* or *Betula pendula* Roth), often in the form of large shrubs, unsuitable for the inference of information about past avalanche events.

5.3. Increase in avalanche frequency over the last decades

Despite the hypothetical limitations in reconstructing high-magnitude snow avalanches that would potentially have destroyed the forest stand in or at the vicinity of the main channels, we are rather confident that our reconstructions include a much smaller amount of noise than more conventional approaches. Interestingly, a clear temporal trend is observed in the reconstructions at each path, with 80% of the events being reconstructed during the 20th century and 25 out of 43 events since 1950.

This observation is in line with the clear increase in the total number of growth disturbances identified at each path since the mid-20th century as well as with a temporal shift in the 50-yr distribution of GDs, i.e. an increasing frequency of traumatic resin ducts, compression wood, callus tissues, and injuries (intensities 2, 3, 4) and a decreasing proportion of growth suppressions (Fig. 6b). This trend toward higher activity since the beginning of the 20th century at Oberwald can be explained reasonably by the fact that a large proportion of growth suppressions, very frequently observed

in the GD spectra during the 19th century, were disregarded from analysis due to the possible confusions between snow avalanche, climatic, and LBM signals. In addition, the overrepresentation of CTs, TRDs and injuries—not attributable to external signals—has probably facilitated the detection of events over the last decades. This bias is frequently observed in dendrogeomorphic reconstructions and mainly attributed to the effect of hidden scars. Because conifer trees mask scars of past events effectively, the existence and/or position of old scars can often not be detected on the stem surface (Stoffel and Perret, 2006), rendering the determination of suitable sample positions a difficult task (Trappmann and Stoffel, 2013). Older events can therefore be missed on increment cores of *L. decidua*, and older trees will tend to yield data on fewer impacts relative to their age which in turn affect return periods for the recent decades. On the other hand, the sampling of trees with visible scars will lead to a facilitated detection of the most recent events.

6. Conclusions

In this study, we used dendrogeomorphic techniques to document past avalanche activity in five avalanche paths at Oberwald (Swiss Alps) with the specific purpose to disentangle signals related to snow avalanche from other ecological disturbances. Based on a 4-step procedure including series of larch budmoth outbreaks and climatic extremes available for the Swiss Alps, 43 avalanche events were reconstructed at Oberwald, whereas 31 events were rejected from the final reconstruction due to potentially strong interferences between the different types of signals. This rejection rate demonstrates the importance of noise in classical, tree-ring based snow avalanche studies and the absolute necessity to discriminate, in future work, ecological from geomorphic disturbances. This is all the more so crucial in mountain environments where a high proportion of dendrogeomorphic studies has been based on larch trees, a species which is cyclically affected by larch budmoth outbreaks. The stringency of our procedure has resulted in the elimination of a large proportion of growth suppression signals which are very frequent in the spectra of growth disturbances, particularly during the 19th century. In this respect, the low level of confidence attributed to a majority of the detected events is interpreted the result of (i) unconfined low-magnitude events at OB1/OB2, and (ii) the limitations of dendrogeomorphic event detection in channelized paths (OB3/OB4) where ancient avalanches can only be reconstructed from surviving marginal trees. Similarly, the rather limited avalanche activity that we reconstruct for the coldest decades of the Little Ice Age and the clear increase in event frequencies since the mid-20th century should not be seen as

Table 4

Synthesis of dendrogeomorphic studies using growth disturbances in tree-ring series to reconstruct past snow avalanche activity. Almost one-fourth (22.9%) of the studies published after the year 2000 utilized European larch (*Larix decidua* Mill.).

Authors and year	Location/country	Number of paths	Species	Sample size	Period	Number of growth disturbances	Minimal Index value	Number of avalanches events
Potter (1969)	Wyoming (USA)	5	<i>Abies lasiocarpa</i> , <i>Pinus albicaulis</i>	50	1963	50	Not computed	1
Schaerer (1972)	British Columbia (Canada)	Not provided	Not provided	Not provided	Not provided	Not provided	Not computed	Unknown
Smith (1973)	Washington (USA)	13	Not provided	Not provided	Not provided	Not provided	Not computed	Unknown
Ives et al. (1976)	Colorado (USA)	Not provided	<i>Populus tremuloides</i> , <i>Picea engelmannii</i>	Not provided	1860–1974	56	Not computed	6
Butler (1979)	Montana (USA)	Not provided	Not provided	Not provided	Not provided	Not provided	Not computed	Not provided
Carrara (1979)	Colorado (USA)	Not provided	<i>Populus tremuloides</i> , <i>Picea engelmannii</i> , <i>Abies lasiocarpa</i>	50	1880–1796	Not provided	Not computed	4
Butler and Malanson (1985)	Montana (USA)	2	<i>Picea engelmannii</i> , <i>Abies lasiocarpa</i> , <i>Pseudotsuga menziesii</i> , <i>Larix occidentalis</i> , <i>Pinus contorta</i>	30 + 48	1924–1979 1934–1981	Not provided	40%	10 + 15
Bryant et al. (1989)	Colorado (USA)	3	<i>Populus tremuloides</i> , <i>Picea engelmannii</i>	60 + 60 + 60	Not provided	Not provided	Not provided	Unknown
Rayback (1998)	Colorado (USA)	2	<i>Abies lasiocarpa</i> , <i>Picea engelmannii</i>	60	1838–1996	Not provided	Not computed	30
Larocque et al. (2001)	Québec (Canada)	1	<i>Picea glauca</i> , <i>Picea mariana</i> , <i>Abies balsamea</i> , <i>Larix laricina</i>	111	1885–2000	Not provided	10%	3
Boucher et al. (2003)	Québec (Canada)	1	<i>Abies balsamea</i> , <i>Picea mariana</i>	62	1895–1996	Not provided	10%	35
Hebertson and Jenkins (2003)	Utah (USA)	16	<i>Picea engelmannii</i> , <i>Abies lasiocarpa</i>	297 (8–26)	1928–1996	Not provided	Not provided	14
Dubé et al. (2004)	Québec (Canada)	3	<i>Thuja occidentalis</i> , <i>Abies balsamea</i> , <i>Betula papyrifera</i>	62 + 20 + 28	1871–1996	Not provided	10%	7
Jenkins and Hebertson (2004)	Utah (USA)	1	<i>Picea engelmannii</i> , <i>Abies concolor</i> , <i>Populus tremuloides</i>	78	1891–1995	Not provided	Not provided	13
Kajimoto et al. (2004)	Not provided (Japan)	1	<i>Abies mariesii</i>	34	Not provided	Not provided	Not computed	Not computed
Muntán et al. (2004)	Pyrenees (Spain)	1	<i>Pinus uncinata</i>	230	1750–2000	Not provided	Not provided	3
Germain et al. (2005)	Québec (Canada)	2	Not provided	78 + 52	1941–2004	420	Not provided	11
Pederson et al. (2006)	Montana (USA)	1	<i>Pseudotsuga menziesii</i>	109	1910–2003	Not provided	10%	27
Stoffel et al. (2006)	Alps (Switzerland)	1	<i>Larix decidua</i>	251	1750–2002	561	Not computed	9
Casteller et al. (2007)	Alps (Switzerland)	2	<i>Larix decidua</i> , <i>Picea abies</i>	66 + 79	Not provided	Not provided	Not computed	Not computed
Mundo et al. (2007)	Andes (Argentina)	1	<i>Nothofagus pumilio</i>	20	Not provided	Not provided	Not computed	Not computed
Butler and Sawyer (2008)	Colorado (USA)	2	<i>Abies lasiocarpa</i> , <i>Pseudotsuga menziesii</i> , <i>Pinus contorta</i>	10 + 12	1945–2008 1963–2008	Not provided	20%, 40%	15 + 9
Casteller et al. (2008)	Andes (Argentina)	1	<i>Nothofagus pumilio</i>	50	Not provided	Not provided	Not computed	6
Reardon et al. (2008)	Montana (USA)	1	<i>Pseudotsuga menziesii</i>	109	1910–2003	Not provided	10%	27
Germain et al. (2009)	Québec (Canada)	12	Not provided	10–243	1895–1999	51–799	10%	19
Laxton and Smith (2009)	Himalaya (India)	1	<i>Cedrus deodara</i>	36	1972–2006	Not provided	Not computed	4
Muntán et al. (2009)	Pyrenees (Spain)	6	<i>Pinus uncinata</i>	26–131	1870–2000	Not provided	16–40%	3
Corona et al. (2010)	Alps (France)	1	<i>Larix decidua</i>	232	1611–1994	901	10%	20
Köse et al. (2010)	Kayaarka (Turkey)	2	<i>Abies bornmuelleriana</i>	61	Not provided	Not provided	Not computed	Not computed
Garavaglia and Pelfini (2011)	Alps (Italia)	71	<i>Picea abies</i>	71–17	1867–2007	854	Not computed	Not computed
Casteller et al. (2011)	Andes (Argentina)	9	<i>Nothofagus pumilio</i>	6–15	1820–2005	Not provided	Not computed	6
Kogelnig-Mayer et al. (2011)	Tyrol (Austria)	1	<i>Picea abies</i>	372	1869–2009	547	2 (Wit)	17
Corona et al. (2012)	Alps (France)	1	<i>Larix decidua</i> , <i>Picea abies</i>	209	1771–2010	645	Variable	34

(continued on next page)

Table 4 (continued)

Authors and year	Location/country	Number of paths	Species	Sample size	Period	Number of growth disturbances	Minimal Index value	Number of avalanches events
Decaulne et al. (2012)	Fnjóskadalur valley (Iceland)	1	<i>Betula pubescens</i>	39	1900–2010	302	40%	5 + 47
Corona et al. (2013)	Queyras (France)	1	<i>Larix decidua</i>	163	1338–2010	514	5%	38
Voiculescu and Onaca (2013)	Bucegi mountains (Romania)	1	<i>Picea abies, Larix ecidua</i>	62	1954–2011	124	Variable	33
Decaulne et al. (2014)	Nordfjord (Norway)	1	<i>Betula pubescens, Alnus incana</i>	91	1900–2011	502	10%	26 + 5
Voiculescu and Onaca (2014)	Bucegi mountains (Romania)	2	<i>Picea abies, Larix ecidua</i>	108	1963–2011	171	Variable	32
Chiroiu et al. (2015)	Fagaras mountains (Romania)	1	<i>Picea abies</i>	105	1852–2013	534	Variable	15–20
Martin and Germain (2016a)	White Mountains (Canada)	6	<i>Abies balsamea, Populus tremuloides, Betula papyrifera, Tsuga canadensis</i>	450	1939–2012	2251	Variable	54
Martin and Germain (2016b)	White Mountains (Canada)	4	<i>Abies balsamea</i>	293	1865–2015	1233	10%	Unknown
Pop et al. (2016)	Southern Carpathians (Romania)	1	<i>Picea abies</i>	57	1900–2013	226	10%	12
Voiculescu et al. (2016)	Fagaras mountains (Romania)	4	<i>Picea abies</i>	293	1867–2012	853	10%	77
Favillier et al. (this study)	Valais, Goms (Switzerland)	5	<i>Larix decidua, Picea abies</i>	566	1780–2013	2389	Variable	48

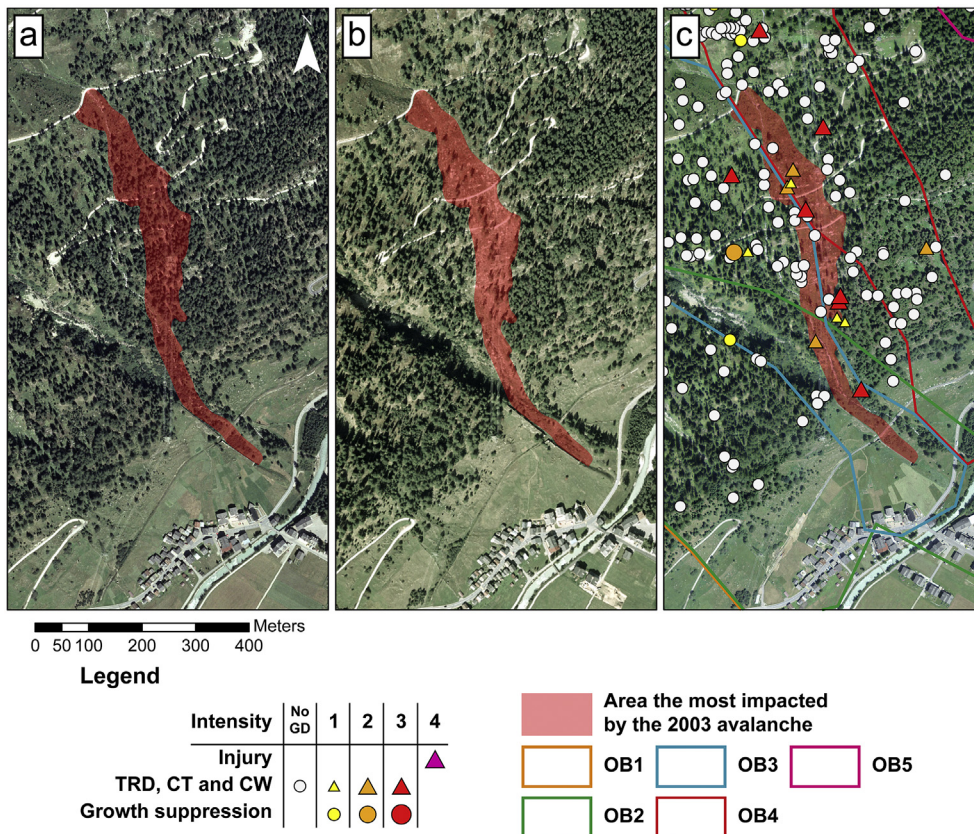


Fig. 11. (a, b) Diachronic evolution of the forest at Oberwald between 1999 and 2005. (c), tree-ring-based reconstruction of the 2003 avalanche event.

climatically-driven variations, but more probably result from an overrepresentation of scars and tangential rows of traumatic resin ducts in the GD spectra for the last decades, representing a sampling bias.

Acknowledgements

The authors acknowledge the Forest and Landscape Department at the Canton of Valais and the Community of Obergoms for financial support.

References

- Alestalo, J., 1971. Dendrochronological interpretation of geomorphic processes. *Fennia* 105, 1–139.
- Ancey, C., 2012. Are there “dragon-kings” events (i.e. genuine outliers) among extreme avalanches? *Eur. Phys. J. Spec. Top.* 205, 117–129. <http://dx.doi.org/10.1140/epjst/e2012-01565-7>.
- Baltensweiler, W., Benz, G., Bovey, P., Delucchi, V., 1977. Dynamics of larch bud moth populations. *Annu. Rev. Entomol.* 22, 79–100. <http://dx.doi.org/10.1146/annurev.en.22.010177.000455>.
- Battipaglia, G., Frank, D., Büntgen, U., Dobrovolný, P., Brázdil, R., Pfister, C., Esper, J., 2010. Five centuries of Central European temperature extremes reconstructed from tree-ring density and documentary evidence. *Glob. Planet. Change* 72, 182–191. <http://dx.doi.org/10.1016/j.gloplacha.2010.02.004>.
- Boucher, D., Filion, L., Hétu, B., 2003. Reconstitution dendrochronologique et fréquence des grosses avalanches de neige dans un couloir subalpin du mont Hog's Back, en Gaspésie centrale (Québec). *Géogr. Phys. Quat.* 57, 159–168. <http://dx.doi.org/10.7202/011311ar>.
- Bryant, C.L., Butler, D.R., Vitek, J.D., 1989. A statistical analysis of tree-ring dating in conjunction with snow avalanches: comparison of on-path versus off-path responses. *Environ. Geol. Water Sci.* 14, 53–59. <http://dx.doi.org/10.1007/BF01740585>.
- Büntgen, U., Esper, J., Frank, D.C., Nicolussi, K., Schmidhalter, M., 2005. A 1052-year tree-ring proxy for Alpine summer temperatures. *Clim. Dyn.* 25, 141–153. <http://dx.doi.org/10.1007/s00382-005-0028-1>.
- Büntgen, U., Frank, D., Liebhold, A., Johnson, D., Carrer, M., Urbinati, C., Grabner, M., Nicolussi, K., Levanic, T., Esper, J., 2009. Three centuries of insect outbreaks across the European Alps. *New Phytol.* 182, 929–941. <http://dx.doi.org/10.1111/j.1469-8137.2009.02825.x>.
- Butler, D.R., 1979. Snow avalanche path terrain and vegetation, glacier National Park, Montana. *Arct. Alp. Res.* 11, 17–32. <http://dx.doi.org/10.2307/1550456>.
- Butler, D.R., Malanson, G.P., 1985. A history of high-magnitude snow avalanches, Southern glacier National Park, Montana, U.S.A. *Mt. Res. Dev.* 5, 175–182. <http://dx.doi.org/10.2307/3673256>.
- Butler, D.R., Sawyer, C.F., 2008. Dendrogeomorphology and high-magnitude snow avalanches: a review and case study. *Nat. Hazards Earth Syst. Sci.* 8, 303–309. <http://dx.doi.org/10.5194/nhess-8-303-2008>.
- Carrara, P.E., 1979. The determination of snow avalanche frequency through tree-ring analysis and historical records at Ophir. *Colo. Geol. Soc. Am. Bull.* 90, 773–780. [http://dx.doi.org/10.1130/0016-7606\(1979\)90<773:TDSOAF>2.0.CO;2](http://dx.doi.org/10.1130/0016-7606(1979)90<773:TDSOAF>2.0.CO;2).
- Casteller, A., Stöckli, V., Villalba, R., Mayer, A.C., 2007. An evaluation of dendroecological indicators of snow avalanches in the Swiss alps. *Arct. Antarct. Alp. Res.* 39, 218–228. [http://dx.doi.org/10.1657/1523-0430\(2007\)39\[218:AEODIO\]2.0.CO;2](http://dx.doi.org/10.1657/1523-0430(2007)39[218:AEODIO]2.0.CO;2).
- Casteller, A., Christen, M., Villalba, R., Martínez, H., Stöckli, V., Leiva, J.C., Bartelt, P., 2008. Validating numerical simulations of snow avalanches using dendrochronology: the Cerro Ventana event in Northern Patagonia, Argentina. *Nat. Hazards Earth Syst. Sci.* 8, 433–443.
- Casteller, A., Villalba, R., Araneo, D., Stöckli, V., 2011. Reconstructing temporal patterns of snow avalanches at Lago del Desierto, Southern Patagonian Andes. *Cold Reg. Sci. Technol.* 67, 68–78. <http://dx.doi.org/10.1016/j.coldregions.2011.02.001>.
- Chiroiu, P., Stoffel, M., Onaca, A., Urdea, P., 2015. Testing dendrogeomorphic approaches and thresholds to reconstruct snow avalanche activity in the Făgăraș mountains (Romanian Carpathians). *Quat. Geochronol.* 27, 1–10. <http://dx.doi.org/10.1016/j.quageo.2014.11.001>.
- Christen, M., Kowalski, J., Bartelt, P., 2010. RAMMS: numerical simulation of dense snow avalanches in three-dimensional terrain. *Cold Reg. Sci. Technol.* 63, 1–14. <http://dx.doi.org/10.1016/j.coldregions.2010.04.005>.
- Cook, E., 1987. The decomposition of tree-ring series for environmental studies. *Tree-Ring Bull.* 47, 37–59.
- Corona, C., Rovéra, G., Lopez Saez, J., Stoffel, M., Perfettini, P., 2010. Spatio-temporal reconstruction of snow avalanche activity using tree rings: pierres jean jeanne avalanche talus, Massif de l'Oisans, France. *Catena* 83, 107–118. <http://dx.doi.org/10.1016/j.catena.2010.08.004>.
- Corona, C., Lopez Saez, J., Stoffel, M., Bonnefoy, M., Richard, D., Astrade, L., Berger, F., 2012. How much of the real avalanche activity can be captured with tree rings? An evaluation of classic dendrogeomorphic approaches and comparison with historical archives. *Cold Reg. Sci. Technol.* 74–75, 31–42. <http://dx.doi.org/10.1016/j.coldregions.2012.01.003>.
- Corona, C., Saez, J.L., Stoffel, M., Rovéra, G., Edouard, J.-L., Berger, F., 2013. Seven centuries of avalanche activity at Echalp (Queyras massif, southern French Alps) as inferred from tree rings. *Holocene* 23 (2), 292–304. <http://dx.doi.org/10.1177/0959683612460784>.
- Coutts, M.P., 1983. Root architecture and tree stability. *Plant Soil* 71, 171–188. <http://dx.doi.org/10.1007/BF02182653>.
- Decaulne, A., Eggertsson, Ó., Sæmundsson, Þ., 2012. A first dendrogeomorphologic approach of snow avalanche magnitude–frequency in Northern Iceland. *Geomorphology* 167–168, 35–44. <http://dx.doi.org/10.1016/j.geomorph.2011.11.017>.
- Decaulne, A., Eggertsson, Ó., Laute, K., Beylich, A.A., 2014. A 100-year extreme snow-avalanche record based on tree-ring research in upper Bødalen, inner Nordfjord, Western Norway. *Geomorphology* 218, 3–15. <http://dx.doi.org/10.1016/j.geomorph.2013.12.036>.
- Dubé, S., Filion, L., Hétu, B., 2004. Tree-ring reconstruction of high-magnitude snow avalanches in the northern Gaspé Peninsula, Québec, Canada. *Arct. Antarct. Alp. Res.* 36, 555–564. [http://dx.doi.org/10.1657/1523-0430\(2004\)036\[0555:TROHSA\]2.0.CO;2](http://dx.doi.org/10.1657/1523-0430(2004)036[0555:TROHSA]2.0.CO;2).
- Efthymiadis, D., Jones, P.D., Briffa, K.R., Auer, I., Böhm, R., Schöner, W., Frei, C., Schmidli, J., 2006. Construction of a 10-min-gridded precipitation data set for the Greater Alpine region for 1800–2003. *J. Geophys. Res.* 111. <http://dx.doi.org/10.1029/2005JD006120>.
- Esper, J., Büntgen, U., Frank, D.C., Nievergelt, D., Liebhold, A., 2007. 1200 years of regular outbreaks in alpine insects. *Proc. R. Soc. B Biol. Sci.* 274, 671–679. <http://dx.doi.org/10.1098/rspb.2006.0191>.
- ESRI, 2013. ArcGIS 10.2.1. ESRI, Redlands, CA.
- Frazer, G.H., 1985. Dendrogeomorphic Evaluation of Snow Avalanche History at Two Sites in Banff National Park. Department of Geography, University of Western Ontario, London, ON, Canada.
- Garavaglia, V., Pelfini, M., 2011. The role of border areas for dendrochronological investigations on catastrophic snow avalanches: a case study from the Italian Alps. *CATENA* 87, 209–215. <http://dx.doi.org/10.1016/j.catena.2011.06.006>.
- George, J.-P., Grabner, M., Karanitsch-Ackerl, S., Mayer, K., Weißbacher, L., Schueler, S., 2016. Genetic variation, phenotypic stability, and repeatability of drought response in European larch throughout 50 years in a common garden experiment. *Tree Physiol.* <http://dx.doi.org/10.1093/treephys/tpw085>.
- Germain, D., 2016. A statistical framework for tree-ring reconstruction of high-magnitude mass movements: case study of snow avalanches in Eastern Canada. *Geogr. Ann. Ser. Phys. Geogr.* <http://dx.doi.org/10.1111/geoa.12138>.
- Germain, D., Filion, L., Hétu, B., 2005. Snow avalanche activity after fire and logging disturbances, Northern Gaspé Peninsula, Quebec, Canada. *Can. J. Earth Sci.* 42, 2103–2116.
- Germain, D., Filion, L., Hétu, B., 2009. Snow avalanche regime and climatic conditions in the Chic-Choc Range, Eastern Canada. *Clim. Change* 92, 141–167. <http://dx.doi.org/10.1007/s10584-008-9439-4>.
- Gruber, U., Bartelt, P., 2007. Snow avalanche hazard modelling of large areas using shallow water numerical methods and GIS. *Environ. Model. Softw.* 22, 1472–1481. <http://dx.doi.org/10.1016/j.envsoft.2007.01.001>.
- Hebertson, E.G., Jenkins, M.J., 2003. Historic climate factors associated with major avalanche years on the Wasatch Plateau, Utah. *Cold Reg. Sci. Technol.* 37, 315–332. [http://dx.doi.org/10.1016/S0165-232X\(03\)00073-9](http://dx.doi.org/10.1016/S0165-232X(03)00073-9).
- Ives, J.D., Mears, A.L., Carrara, P.E., Bovis, M.J., 1976. Natural hazards in mountain Colorado. *Ann. Assoc. Am. Geogr.* 66, 129–144. <http://dx.doi.org/10.1111/j.1467-8306.1976.tb01076.x>.
- Jenkins, M.J., Hebertson, E.G., 2004. A practitioner's guide for using dendroecological techniques to determine the extent and frequency of avalanches. In: *International Snow Science Workshop*, pp. 423–434.
- Johnson, E.A., 1987. The relative importance of snow avalanche disturbance and thinning on canopy plant populations. *Ecology* 68, 43. <http://dx.doi.org/10.2307/1938803>.
- Kajimoto, T., Daimaru, H., Okamoto, T., Otani, T., Onodera, H., 2004. Effects of snow avalanche disturbance on regeneration of subalpine *Abies mariesii* forest, Northern Japan. *Arct. Antarct. Alp. Res.* 36, 436–445.
- Kennedy, M.D., 2013. Introducing Geographic Information Systems with ArcGIS: a Workbook Approach to Learning GIS. John Wiley & Sons.
- Kogelnig-Mayer, B., Stoffel, M., Schneuwly-Bollschweiler, M., Hübl, J., Rudolf-Miklau, F., 2011. Possibilities and limitations of dendrogeomorphic time-series reconstructions on sites influenced by debris flows and frequent snow avalanche activity. *Arct. Antarct. Alp. Res.* 43, 649–658. <http://dx.doi.org/10.1657/1938-4246-43.4.649>.
- Kogelnig-Mayer, B., Stoffel, M., Schneuwly-Bollschweiler, M., 2013. Four-dimensional growth response of mature *Larix decidua* to stem burial under natural conditions. *Trees* 27, 1217–1223. <http://dx.doi.org/10.1007/s00468-013-0870-4>.
- Köse, N., Aydın, A., Akkemik, Ü., Yurtseven, H., Güner, T., 2010. Using tree-ring signals and numerical model to identify the snow avalanche tracks in Kastamonu. *Turk. Nat. Hazards* 54, 435–449. <http://dx.doi.org/10.1007/s11069-009-9477-x>.
- Kress, A., Saurer, M., Büntgen, U., Treyde, K.S., Bugmann, H., Siegwolf, R.T.W., 2009. Summer temperature dependency of larch budmoth outbreaks revealed by Alpine tree-ring isotope chronologies. *Oecologia* 160, 353–365. <http://dx.doi.org/10.1007/s00442-009-1290-4>.
- Larocque, S.J., Hétu, B., Filion, L., 2001. Geomorphic and dendroecological impacts of slushflows in central Gaspé Peninsula (Québec, Canada). *Geogr. Ann. Ser. Phys. Geogr.* 83, 191–201. <http://dx.doi.org/10.1111/j.0435-3676.2001.00154.x>.
- Latenser, M., Pfister, C., 1997. Avalanches in Switzerland 1500–1990. In: Frenzel, B., Matthews, J., Gläser, A., Weiss, M. (Eds.), *Rapide Mass Movement since the*

- Holocene., *Palaeoclimate Research*, pp. 241–266.
- Laxton, S.C., Smith, D.J., 2009. Dendrochronological reconstruction of snow avalanche activity in the Lahul Himalaya, Northern India. *Nat. Hazards* 49, 459–467. <http://dx.doi.org/10.1007/s11069-008-9288-5>.
- Lévesque, M., Saurer, M., Siegwolf, R., Eilmann, B., Brang, P., Bugmann, H., Rigling, A., 2013. Drought response of five conifer species under contrasting water availability suggests high vulnerability of Norway spruce and European larch. *Glob. Change Biol.* <http://dx.doi.org/10.1111/gcb.12268> n/a-n/a.
- Martin, J.-P., Germain, D., 2016a. Dendrogeomorphic reconstruction of snow avalanche regime and triggering weather conditions: a classification tree model approach. *Prog. Phys. Geogr.* 40, 527–548. <http://dx.doi.org/10.1177/0309133315625863>.
- Martin, J.-P., Germain, D., 2016b. Can we discriminate snow avalanches from other disturbances using the spatial patterns of tree-ring response? Case studies from the Presidential Range, White Mountains, New Hampshire, United States. *Dendrochronologia* 37, 17–32. <http://dx.doi.org/10.1016/j.dendro.2015.12.004>.
- Mundo, I.A., Barrera, M.D., Roig, F.A., 2007. Testing the utility of *Nothofagus pumilio* for dating a snow avalanche in Tierra del Fuego, Argentina. *Dendrochronologia* 25, 19–28. <http://dx.doi.org/10.1016/j.dendro.2007.01.001>.
- Muntán, E., Andreu, L., Oller, P., Gutiérrez, E., Martínez, P., 2004. Dendrochronological study of the Canal del Roc Roig avalanche path: first results of the Aludex project in the Pyrenees. *Ann. Glaciol.* 38, 173–179. <http://dx.doi.org/10.3189/172756404781815077>.
- Muntán, E., García, C., Oller, P., Martí, G., García, A., Gutiérrez, E., 2009. Reconstructing snow avalanches in the Southeastern Pyrenees. *Nat. Hazards Earth Syst. Sci.* 9, 1599–1612.
- Pederson, G.T., Reardon, B.A., Caruso, C.J., Fagre, D.B., 2006. High resolution tree-ring based spatial reconstructions of snow avalanche activity in Glacier National Park, Montana, USA. In: *Proceedings of the International Snow Science Workshop ISSW*. Citeseer, pp. 436–443.
- Peltola, H., Kellomäki, S., Väisänen, H., Ilkonen, V.-P., 1999. A mechanistic model for assessing the risk of wind and snow damage to single trees and stands of Scots pine, Norway spruce, and birch. *Can. J. For. Res.* 29, 647–661. <http://dx.doi.org/10.1139/x99-029>.
- Pop, O.T., Gavrilă, I.-G., Roșian, G., Meseșan, F., Decaulne, A., Holobacă, I.H., Anghel, T., 2016. A century-long snow avalanche chronology reconstructed from tree-rings in Parâng Mountains (Southern Carpathians, Romania). *Quatern. Int.* 415, 230–240. <http://dx.doi.org/10.1016/j.quaint.2015.11.058>.
- Potter, N., 1969. Tree-ring dating of snow avalanche tracks and the geomorphic activity of avalanches, northern Absaroka Mountains, Wyoming, Boulder, CO. *Geol. Soc. Am. Spec. Pap.* 123, 141–165.
- Rayback, S.A., 1998. A dendrogeomorphological analysis of snow avalanches in the Colorado front range. *Usa. Phys. Geogr.* 19, 502–515. <http://dx.doi.org/10.1080/02723646.1998.10642664>.
- Reardon, B.A., Pederson, G.T., Caruso, C.J., Fagre, D.B., 2008. Spatial reconstructions and comparisons of historic snow avalanche frequency and extent using tree rings in glacier National Park, Montana, U.S.A. *Arct. Antarct. Alp. Res.* 40, 148–160. [http://dx.doi.org/10.1657/1523-0430\(06-069\)\[REARDON\]2.0.CO;2](http://dx.doi.org/10.1657/1523-0430(06-069)[REARDON]2.0.CO;2).
- Rudolf-Miklau, F., Sauermoser, S., Mears, A.I., Boensch, M.M., 2015. *The Technical Avalanche Protection Handbook*.
- Schaerer, P.A., 1972. Terrain and vegetation of snow avalanche sites at Rogers Pass, British Columbia in mountain geomorphology. In: Slaymaker, O., McPherson, H.J. (Eds.), *Mountain Geomorphology: Geomorphological Processes in the Canadian Cordillera*, pp. 215–222. Vancouver B.C.
- Schläpky, R., Jomelli, V., Grancher, D., Stoffel, M., Corona, C., Brunstein, D., Eckert, N., Deschatres, M., 2013. A new tree-ring-based, semi-quantitative approach for the determination of snow avalanche events: use of classification trees for validation. *Arct. Antarct. Alp. Res.* 45, 383–395. <http://dx.doi.org/10.1657/1938-4246-45.3.383>.
- Schneuwly, D.M., Stoffel, M., Bollschweiler, M., 2009a. Formation and spread of callus tissue and tangential rows of resin ducts in *Larix decidua* and *Picea abies* following rockfall impacts. *Tree Physiol.* 29, 281–289. <http://dx.doi.org/10.1093/treephys/tpn026>.
- Schneuwly, D.M., Stoffel, M., Dorren, L.K.A., Berger, F., 2009b. Three-dimensional analysis of the anatomical growth response of European conifers to mechanical disturbance. *Tree Physiol.* 29, 1247–1257. <http://dx.doi.org/10.1093/treephys/tpp056>.
- Shroder, J., 1978. Dendrogeomorphological analysis of mass movement on table cliffs plateau, Utah. *Quat. Res.* 9, 168–185. [http://dx.doi.org/10.1016/0033-5894\(78\)90065-0](http://dx.doi.org/10.1016/0033-5894(78)90065-0).
- Silhán, K., Stoffel, M., 2015. Impacts of age-dependent tree sensitivity and dating approaches on dendrogeomorphic time series of landslides. *Geomorphology* 236, 34–43. <http://dx.doi.org/10.1016/j.geomorph.2015.02.003>.
- Smith, L., 1973. Indication of snow avalanche periodicity through interpretation of vegetation patterns in the North Cascades, Washington. In: *Methods of Avalanche Control on Washington Mountain Highways - Third Annual Report*, pp. 55–101. Washington State Highway Department: Research Program Report 8.4.
- Stoffel, M., 2008. Dating past geomorphic processes with tangential rows of traumatic resin ducts. *Dendrochronologia* 26 (1), 53–60.
- Stoffel, M., Perret, S., 2006. Reconstructing past rockfall activity with tree rings: some methodological considerations. *Dendrochronologia* 24, 1–15. <http://dx.doi.org/10.1016/j.dendro.2006.04.001>.
- Stoffel, M., Bollschweiler, M., 2008. Tree-ring analysis in natural hazards research - an overview. *Nat. Hazards Earth Syst. Sci.* 8, 187–202. <http://dx.doi.org/10.5194/nhess-8-187-2008>.
- Stoffel, M., Hitz, O.M., 2008. Snow avalanche and rockfall impacts leave different anatomical signatures in tree rings of *Larix decidua*. *Tree Physiol.* 28 (11), 1713–1720.
- Stoffel, M., Corona, C., 2014. Dendroecological dating of geomorphic disturbance in trees. *Tree-Ring Res.* 70, 3–20. <http://dx.doi.org/10.3959/1536-1098-70.1.3>.
- Stoffel, M., Lievre, L., Monbaron, M., Perret, S., 2005. Seasonal timing of rockfall activity on a forested slope at Täsch (Swiss Alps) – a dendrochronological approach. *Z. Für Geomorphol.* 49, 89–106.
- Stoffel, M., Bollschweiler, M., Hassler, G.-R., 2006. Differentiating past events on a cone influenced by debris-flow and snow avalanche activity – a dendrogeomorphological approach. *Earth Surf. Process. Landf.* 31, 1424–1437. <http://dx.doi.org/10.1002/esp.1363>.
- Stoffel, M., Bollschweiler, M., Butler, D.R., Luckman, B., 2010. *Tree Rings and Natural Hazards*. Springer, Dordrecht; New York.
- Stoffel, M., Butler, D.R., Corona, C., 2013. Mass movements and tree rings: a guide to dendrogeomorphic field sampling and dating. *Geomorphology* 200, 106–120. <http://dx.doi.org/10.1016/j.geomorph.2012.12.017>.
- Stucki, P., Brönnimann, S., Martius, O., Welker, C., Imhof, M., von Wattenwyl, N., Philipp, N., 2014. A catalog of high-impact windstorms in Switzerland since 1859. *Nat. Hazards Earth Syst. Sci.* 14, 2867–2882. <http://dx.doi.org/10.5194/nhess-14-2867-2014>.
- Trappmann, D., Stoffel, M., 2013. Counting scars on tree stems to assess rockfall hazards: a low effort approach, but how reliable? *Geomorphology* 180–181, 180–186. <http://dx.doi.org/10.1016/j.geomorph.2012.10.009>.
- Usbeck, T., Wohlgemuth, T., Pfister, C., Volz, R., Beniston, M., Dobbertin, M., 2009. Wind speed measurements and forest damage in Canton Zurich (Central Europe) from 1891 to winter 2007. *Int. J. Climatol.* <http://dx.doi.org/10.1002/joc.1895> n/a-n/a.
- Van der Burght, L., Stoffel, M., Bigler, C.J., 2012. Analysis and modelling of tree succession on a recent rockslide deposit. *Plant Ecol.* 213, 35–46.
- Voiculescu, M., Onaca, A., 2013. Snow avalanche assessment in the Sinaia ski area (Bucegi Mountains, Southern Carpathians) using the dendrogeomorphology method. *Area* 45, 109–122. <http://dx.doi.org/10.1111/area.12003>.
- Voiculescu, M., Onaca, A., 2014. Spatio-temporal reconstruction of snow avalanche activity using dendrogeomorphological approach in Bucegi Mountains Romanian Carpathians. *Cold Reg. Sci. Technol.* 104–105, 63–75. <http://dx.doi.org/10.1016/j.coldregions.2014.04.005>.
- Voiculescu, M., Onaca, A., Chiroiu, P., 2016. Dendrogeomorphic reconstruction of past snow avalanche events in Bălea glacial valley–Făgăraș massif (Southern Carpathians), Romanian Carpathians. *Quatern. Int.* 415, 286–302. <http://dx.doi.org/10.1016/j.quaint.2015.11.115>.
- Weber, U.M., 1997. Dendroecological reconstruction and interpretation of larch budmoth (*Zeiraphera diniana*) outbreaks in two central alpine valleys of Switzerland from 1470–1990. *Trees* 11, 277–290. <http://dx.doi.org/10.1007/PL00009674>.